INSTITUTE OF PHYSICS PUBLISHING NONLINEARITY

Nonlinearity **17** (2004) 711–728 PII: S0951-7715(04)61311-9

Global well-posedness and multi-tone solutions of a class of nonlinear nonlocal cochlear models in hearing*

Jack Xin[1,3] **and Yingyong Qi**[2]

[1] Department of Mathematics and ICES, University of Texas at Austin, Austin, TX 78712, USA
[2] Qualcomm Inc, 5775 Morehouse Drive, San Diego, CA 92121, USA

E-mail: jxin@math.utexas.edu.

Received 21 March 2003, in final form 19 December 2003
Published 27 January 2004
Online at stacks.iop.org/Non/17/711 (DOI: 10.1088/0951-7715/17/2/020)

Recommended by E S Titi

Abstract

We study a class of nonlinear nonlocal cochlear models of the transmission line type, describing the motion of basilar membrane (BM) in the cochlea. They are damped dispersive partial differential equations (PDEs) driven by time dependent boundary forcing due to the input sounds. The global well-posedness in time follows from energy estimates. Uniform bounds of solutions hold in the case of bounded nonlinear damping. When the input sounds are multi-frequency tones, and the nonlinearity in the PDEs is cubic, we construct smooth quasi-periodic solutions (multi-tone solutions) in the weakly nonlinear regime, where new frequencies are generated due to nonlinear interaction. When the input consists of two tones at frequencies f_1, f_2 ($f_1 < f_2$), and high enough intensities, numerical results illustrate the formation of combination tones at $2f_1 - f_2$ and $2f_2 - f_1$, in agreement with hearing experiments. We visualize the frequency content of solutions through the FFT power spectral density of displacement at selected spatial locations on the BM.

Mathematics Subject Classification: 35L05, 35Q72, 35L50, 41A60, 37M05

1. Introduction

Digital signal processing on sounds is an essential component of modern hearing devices [18], and a useful tool for evaluating acoustic theories of peripheral auditory systems [15], among others. A fundamental issue is to model the auditory response to complex tones

* This work was partially supported by ARO grant DAAD 19-00-1-0524, NSF ITR-0219004 and a fellowship from the John Simon Guggenheim Memorial Foundation.
[3] Author to whom any correspondence should be addressed.

because the nonlinear interaction of acoustic waves of different frequencies allows for audio compression [18] among other applications. Nonlinearities are known to originate in the cochlea and are further modified in higher level auditory pathways. The cochlear mechanics has first-principle descriptions, and so partial differential equations (PDEs) become a natural mathematical framework to initiate computation. However, *in vivo* cochlear dynamics is not a purely mechanical problem, and neural feedback is present to modify responses. To incorporate both aspects, a first-principle-based PDE model was studied in [23] for voice signal processing, where the neural aspect is introduced in the model phenomenologically. The first-principle-based PDE approach is more systematic compared with the filter bank method [15], and has shown encouraging results. In [23], time domain computation on multi-tone inputs revealed tonal suppressions in qualitative agreement with earlier neural experimental findings. Though both methods are nonlinear, a major difference between [15] and [23] is that the former simulates the basilar membrane (BM) response at a single site while the latter contains the BM response over its entire length with nearest-neighbour coupling.

In this paper, we shall analyse the well-posedness and construct multi-tone solutions of such PDE models in the form:

$$p_{xx} - Nu_{tt} = \epsilon_s(x)u_t, \qquad x \in (0, L), \tag{1.1}$$

$$p = mu_{tt} + r(x, |u|, |u_t|)u_t + s(x)u, \tag{1.2}$$

where p is the fluid pressure difference across the BM, u the BM displacement, and L the longitudinal length of BM; N is a constant depending on fluid density and cochlear channel size, $\epsilon_s(x) \geqslant 0$ is the damping of longitudinal fluid motion, and m, r and s are the mass, damping and stiffness of BM per unit area, with m a constant and s a continuously differentiable non-negative function of x. The coefficient r is a nonlinear function(al) of x, u, u_t:

$$r(x, |u|, |u_t|) = r_a(|u_t|^2) + \gamma \int_0^L P(|u(x', t)|)K(x - x')\,\mathrm{d}x'. \tag{1.3}$$

Here $r_a(\cdot)$ is the local part of BM damping, a non-negative continuously differentiable monotone increasing function and $r_a(0) > 0$. In the nonlocal BM damping and $K = K(x)$ is a positive localized Lipschitz continuous kernel function with total integral over $x \in R^1$ equal to 1 and $P(\cdot)$ is a non-negative continuously differentiable function such that for some constant $C > 0$

$$P(0) = 0, \qquad P(q) \leqslant C(1 + q^2), \quad \forall q \geqslant 0. \tag{1.4}$$

The nonlinear nonlocal form of damping (1.3) implies that the response at certain location x' (excitation) can increase the damping at a nearby point x, thus inhibiting the response there. Inhibition induced by excitation is observed experimentally in terms of firing rates of auditory neurons under multi-tone sound input, [5, 6]. The nonlinear nonlocal damping, proposed earlier in [14, 9], is an efficient way of extracting the auditory neural feedback to BM and model the nonlinear interactions of complex sounds [4, 23]. The monotonicity of r_a in $|u_t|$ and often of P in $|u|$ is consistent with the reduced sensitivity or compression of BM responses at increasing sound input intensities [19].

The boundary and initial conditions of the system are:

$$p_x(0, t) = T_M p_T(t) \equiv f(t), \qquad p(L, t) = 0, \tag{1.5}$$

$$u(x, 0) = u_0(x), \qquad u_t(x, 0) = u_1(x), \tag{1.6}$$

where the initial data is such that $(u_0, u_1) \in (H^1([0, L]))^2$, $(u_0, u_1)(L) = (0, 0)$; $p_T(t)$ is the input sound pressure at the eardrum and T_M is a bounded linear map modelling the functions of the middle ear, with output depending on the frequency content of $p_T(t)$. If $p_T = \sum_{j=1}^{J_M} A_j \exp\{\mathrm{i}\omega_j t\} + \text{c.c.}$, a multi-tone input, c.c. denoting the complex conjugate, J_M

a positive integer, then $T_M p_T(t) = \sum_{j=1}^{J_M} B_j \exp\{\mathrm{i}\omega_j t\} + \text{c.c.}$, where $B_j = a_M(\omega_j)A_j$ and, $a_M(\cdot)$ a scaling function built from the filtering characteristics of the middle ear [7].

Cochlear modelling has a long history, and various linear models have been studied at length by analytical and numerical methods (see [10, 12] and references therein). A brief derivation of the cochlear model of the transmission line type, e.g. the linear portion of (1.1)–(1.6), is nicely presented in [20] based on fluid and elasticity equations.

It has been realized that nonlinearity is essential for multi-tone interactions [8, 11, 3, 6] etc. Nonlinearity could be introduced phenomenologically based on the spreading of electrical and neural activities between hair cells at different BM locations suggested by experimental data [9, 4]. Such a treatment turned out to be efficient for signal processing purposes [23], and (1.3)–(1.4) is a generalization of existing nonlinearities [9, 4, 21].

Multi-tone solutions require one to perform numerical computations in the time domain. The model system (1.1)–(1.6) is dispersive, and long waves tend to propagate with little decay from the entrance point $x = 0$ (stapes) to the exit $x = L$ (helicotrama). The function $\epsilon_s(x)$ is supported near $x = L$ and its role in numerics is to suck out the long waves accumulating near the exit [23]. In the analysis of model solutions, which are concerned mainly with interior properties, however, we shall set ϵ_s to zero for technical convenience.

Selective positive or negative damping has been a novel way to filter images in the PDE method of image processing (see [17] among others).

The rest of this paper is organized as follows. In section 2, we perform energy estimates of solutions for the model system (1.1)–(1.6), prove the global well-posedness and obtain growth and uniform bounds in Sobolev spaces. In section 3, we construct exact multi-frequency solutions when γ is small enough and nonlinearity is cubic, using contraction mapping in a suitable Banach space. The constructed solutions contain all linear integral combinations of input frequencies. In section 4, for two input tones with frequencies f_1 and f_2 ($f_1 < f_2$), we illustrate numerically the combination tones, $2f_1 - f_2$ and $2f_2 - f_1$, generated on power spectral density plots at selected points on BM. Such tones are heard on musical instruments (piano and violin), known as the Tartini tones discovered by the celebrated Italian composer Giuseppe Tartini [2]. The conclusions are given in section 5.

2. Global well-posedness and estimates

Let us consider the initial boundary value problem (IBVP) defined by (1.1)–(1.6) and show that solutions exist uniquely in $H^1([0, L])$ for all time. To this end, it is convenient to work with the equivalent integral form of the equations. It follows from (1.1) and (1.5) that

$$\begin{aligned} p_x &= \int_0^x (Nu_{tt} + \epsilon_s(x)u_t)\,\mathrm{d}x + f(t), \\ -p(t,x) &= \int_x^L \mathrm{d}x' \int_0^{x'} (Nu_{tt} + \epsilon_s u_t)\,\mathrm{d}x'' + f(t)(L-x). \end{aligned} \tag{2.1}$$

Combining (1.2) and (2.1), we get

$$mu_{tt} + \int_x^L \mathrm{d}x' \int_0^{x'} (Nu_{tt} + \epsilon_s u_t)\,\mathrm{d}x'' + f(t)(L-x) = -r(x, |u|, |u_t|)u_t - s(x)u, \tag{2.2}$$

with initial data (1.6). Let $w = (w_1, w_2) = (u, u_t)$, and write (2.2) in the system form:

$$w_{1,t} = w_2, \tag{2.3}$$

$$\begin{aligned} mw_{2,t} + \int_x^L \mathrm{d}x' \int_0^{x'} Nw_{2,t}\,\mathrm{d}x'' = &- \int_x^L \mathrm{d}x' \int_0^{x'} \epsilon_s w_2\,\mathrm{d}x'' \\ &- r(x, |w_1|, |w_2|)w_2 - s(x)w_1 + f(t)(x-L). \end{aligned} \tag{2.4}$$

The related integral form is

$$\begin{aligned} w_1 &= u_0 + \int_0^t w_2(x,\tau)\,\mathrm{d}\tau, \\ Aw_2 = Au_1 &- \int_0^t \mathrm{d}\tau \int_x^L \mathrm{d}x' \int_0^{x'} \epsilon_s w_2\,\mathrm{d}x'' \\ &- \int_0^t \mathrm{d}\tau r(x,|w_1|,|w_2|)w_2 - s(x)\int_0^t w_1\,\mathrm{d}\tau + (x-L)\int_0^t f(\tau)\,\mathrm{d}\tau, \end{aligned} \tag{2.5}$$

where $A : L^2([0,L]) \to L^2([0,L])$ is a bounded self-adjoint linear operator:

$$Ag \equiv mg + \int_x^L \mathrm{d}x' \int_0^{x'} Ng\,\mathrm{d}x'' \equiv mg + \tilde{A}g. \tag{2.6}$$

To see the self-adjointness of A, let $g, h \in L^2([0,L])$, then $(\tilde{A}g, h) = (g, \tilde{A}h)$ or

$$\begin{aligned} \int_0^L \left(\int_x^L \mathrm{d}x' \int_0^{x'} g(x'')\,\mathrm{d}x''\right) h(x)\,\mathrm{d}x &= \int_0^L \left(\int_x^L \mathrm{d}x' \int_0^{x'} g(x'')\,\mathrm{d}x''\right) \mathrm{d}\int_0^x h \\ &= \int_0^L \left(\int_0^x \mathrm{d}x' g(x')\right)\left(\int_0^x \mathrm{d}x' h(x')\right)\mathrm{d}x, \end{aligned}$$

hence $(Ag, h)_{L^2} = (g, Ah)_{L^2}$. Clearly, A is bounded; also $(A\cdot,\cdot) = (A\cdot,\cdot)_{L^2}$ is an equivalent square L^2 norm:

$$\begin{aligned} &(Ag, g) = m\|g\|_2^2 + N\int_0^L \left(\int_0^x g\right)^2 \mathrm{d}x \geqslant m\|g\|_2^2, \\ &(Ag, g) \leqslant m\|g\|_2^2 + NL^2\|g\|_2^2 = (m + NL^2)\|g\|_2^2. \end{aligned} \tag{2.7}$$

The lower bound in (2.7) implies that A has a bounded inverse [24]. The bounded inverse of A is denoted by A^{-1} below.

Now, we establish the global existence of solutions of (2.3)–(2.4) in the function space $C([0,\infty); (H^1([0,L]))^2)$. It is straightforward to show by the contraction mapping principle that if $\|(u_0,u_1)\|_{H^1} < \infty$, there is a time t_* such that (2.5) has a unique solution in $C([0,t_*); (H^1([0,L]))^2)$ under our assumptions on the nonlinearities. Such a solution in fact lies in $C^1([0,t_*); (H^1([0,L]))^2)$, and obeys the differential form of equations (2.3)–(2.4), with both sides interpreted in the H^1 sense. Taking the limit $x \to L$, we find that the system (2.3)–(2.4) reduces to the ODE system:

$$\begin{aligned} w_{1,t} &= w_2, \\ w_{2,t} &= -r(t)w_2 - s(L)w_1, \end{aligned}$$

with initial data $(w_1, w_2)(L,0) = (0,0)$; hence $(w_1,w_2)(L,t) = (0,0)$, $\forall t \in (0,t_*)$.

Let us derive estimates of solutions in H^1 that are global in time to extend the local solutions to global ones (so $t_* = \infty$). The left-hand side of (2.4) is just $(Aw_2)_t$, and

$$(w_2, (Aw_2)_t) = (w_2, A(w_2)_t) = (Aw_2, w_{2,t}) = (w_{2,t}, Aw_2),$$

therefore,

$$\frac{\mathrm{d}}{\mathrm{d}t}(Aw_2, w_2) = (w_{2,t}, Aw_2) + (Aw_{2,t}, w_2) = 2(w_2, Aw_{2,t}), \tag{2.8}$$

and hence $\frac{1}{2}(\mathrm{d}/\mathrm{d}t)(Aw_2, w_2) = (w_2, Aw_{2,t})$. Multiplying (2.3) by w_1, (2.4) by w_2, adding the two expressions and integrating over $[0,L]$, we estimate, using the Cauchy–Schwarz inequality

and (1.3) that

$$\begin{aligned}(w_1, w_{1,t}) + (w_2, (Aw_2)_t) &= \frac{1}{2}\frac{\mathrm{d}}{\mathrm{d}t}((w_1, w_1) + (Aw_2, w_2)) \\ &= -\left(\int_x^L \mathrm{d}x' \int_0^{x'} \epsilon_s w_2 \,\mathrm{d}x'', w_2\right) - (rw_2, w_2) + (w_2, w_1) - (sw_1, w_2) \\ &\quad +(f(t)(x-L), w_2) \\ &\leqslant -r_a(0)\|w_2\|_2^2 + r_a(0)\|w_2\|_2^2 + \frac{1}{4r_a(0)}\|f(t)(x-L)\|_2^2 \\ &\quad - \int_0^L \left(\int_0^x \epsilon_s w_2\right)\left(\int_0^x w_2\right)\mathrm{d}x + \|(1-s)\|_\infty \|w_2\|_2 \|w_1\|_2 \\ &\leqslant \frac{1}{12r_a(0)}|f(t)|^2 L^3 + L^2\|\epsilon_s\|_2\|w_2\|_2^2 + \frac{1}{2}\|1-s\|_\infty(\|w_1\|_2^2 + \|w_2\|_2^2) \\ &\leqslant \left(\frac{1}{2}\|1-s\|_\infty + L^2\|\epsilon_s\|_2\right)\|w_2\|_2^2 + \frac{1}{2}\|1-s\|_\infty\|w_1\|_2^2 + \frac{1}{12r_a(0)}|f(t)|^2 L^3. \end{aligned} \tag{2.9}$$

Let $C_1 = \max((1/m)\|1-s\|_\infty + (2L^2/m)\|\epsilon_s\|_2, \frac{1}{2}\|1-s\|_\infty)$ and $2E = (w_1, w_1) + (Aw_2, w_2)$; we have from (2.9)

$$\frac{\mathrm{d}E}{\mathrm{d}t} \leqslant C_1 E + \frac{1}{12r_a(0)}|f(t)|^2 L^3, \tag{2.10}$$

or

$$E(t) \leqslant E(0) + C_1 \int_0^t E(s)\,\mathrm{d}s + \frac{L^3}{12r_a(0)}\int_0^t |f|^2(s')\,\mathrm{d}s'.$$

The Gronwall inequality implies

$$E(t) \leqslant \left(E(0) + \frac{L^3}{12r_a(0)}\int_0^t |f|^2(t')\,\mathrm{d}t'\right)\mathrm{e}^{C_1 t},$$

or

$$\|(w_1, w_2)\|_2^2 \leqslant \min(1, m)^{-1}\left(E(0) + \frac{L^3}{12r_a(0)}\int_0^t |f|^2(t')\,\mathrm{d}t'\right)\mathrm{e}^{C_1 t}. \tag{2.11}$$

Next, we obtain the gradient estimates. Differentiating (2.3)–(2.4) with respect to x gives

$$\frac{\mathrm{d}}{\mathrm{d}t}w_{1,x} = w_{2,x}, \tag{2.12}$$

$$\begin{aligned}\frac{\mathrm{d}}{\mathrm{d}t}\left(mw_{2,x} - N\int_0^x w_2(x', \cdot)\,\mathrm{d}x'\right) &= \int_0^x \epsilon_s(x')w_2(x')\,\mathrm{d}x' - rw_{2,x} - s'w_1 - sw_{1,x} + f(t) \\ &\quad -\left(2r_a' w_2 w_{2,x} + \gamma\int_0^L P(w_1)(x', t)K_x(x-x')\,\mathrm{d}x'\right)w_2. \end{aligned} \tag{2.13}$$

Multiplying (2.12) and (2.13) by $w_{1,x}$ and $w_{2,x}$, and integrating over $x \in [0, L]$, we find

$$\begin{aligned}\frac{1}{2}\frac{\mathrm{d}}{\mathrm{d}t}(\|w_{1,x}\|_2^2 + m\|w_{2,x}\|_2^2) &= N\int_0^L w_{2,x}\int_0^x w_{2,t}(x', \cdot)\,\mathrm{d}x' + (w_{1,x}, w_{2,x}) \\ &\quad +\left(w_{2,x}, \int_0^x \epsilon_s w_2\right) - \int_0^L rw_{2,x}^2 - \int_0^L \left(2r_a' w_2 w_{2,x} + \gamma\int_0^L P(w_1)K_x\right) \\ &\quad \times w_2 w_{2,x} - \int_0^L s'w_1 w_{2,x} - \int_0^L sw_{1,x}w_{2,x} + f(t)\int_0^L w_{2,x}. \end{aligned} \tag{2.14}$$

The integral in the first term of the right-hand side of (2.14) can be written as

$$-N\int_0^L w_2 w_{2,t}\,\mathrm{d}x = -\frac{N}{2}\frac{\mathrm{d}}{\mathrm{d}t}\int_0^L w_2^2\,\mathrm{d}x, \tag{2.15}$$

where we applied integration by parts once and $w_2(L,t)=0$.

The other terms are estimated as follows:

$$\begin{aligned}
-\int_0^L \mathrm{d}x\left(\gamma\int_0^L P(w_1)(x',\cdot)K_x(x-x')\,\mathrm{d}x'\right)w_2 w_{2,x}
&\leqslant C\int_0^L |w_2 w_{2,x}|\int_0^L (1+|w_1|^2)|K_x|(x-x')\,\mathrm{d}x'\\
&\leqslant C(1+\|w_1\|_2^2)\int_0^L |w_2 w_{2,x}|\\
&\leqslant C(1+\|w_1\|_2^2)\|w_2\|_2\|w_{2,x}\|_2\\
&\leqslant \delta_0\|w_{2,x}\|_2^2 + \frac{1}{4\delta_0}C^2(1+\|w_1\|_2^2)^2\|w_2\|_2^2,
\end{aligned} \tag{2.16}$$

for any $\delta_0>0$, $C=C(\|K_x\|_\infty)$, by (1.4). Integration by parts and $w_2(L,t)=0$ give

$$\left(w_{2,x},\int_0^x \epsilon_s w_2\right) = -\int_0^L \epsilon_s w_2^2\,\mathrm{d}x \leqslant 0. \tag{2.17}$$

Using the Cauchy–Schwarz inequalities we get

$$-\int_0^L r w_{2,x}^2 - 2\int_0^L r_a' w_2^2 w_{2,x}^2 \leqslant -r_a(0)\|w_{2,x}\|_2^2, \tag{2.18}$$

$$\begin{aligned}
-\int_0^L s' w_1 w_{2,x}\,\mathrm{d}x - \int_0^L s w_{1,x} w_{2,x} + (w_{1,x}, w_{2,x})
&\leqslant \|1-s\|_\infty\|w_{1,x}\|_2\|w_{2,x}\|_2 + \|s'\|_\infty\|w_1\|_2\|w_{2,x}\|_2\\
&\leqslant 2\delta_0\|w_{2,x}\|_2^2 + \frac{1}{16\delta_0}\|1-s\|_\infty^2\|w_{1,x}\|_2^2 + \frac{1}{16\delta_0}\|s'\|_\infty^2\|w_1\|_2^2,
\end{aligned} \tag{2.19}$$

$$f(t)\int_0^L w_{2,x} \leqslant |f(t)|L^{1/2}\|w_{2,x}\|_2 \leqslant \delta_0\|w_{2,x}\|_2^2 + \frac{1}{4\delta_0}|f(t)|^2 L. \tag{2.20}$$

Combining (2.14)–(2.20) with $4\delta_0 = r_a(0)/2$, we get

$$\frac{\mathrm{d}}{\mathrm{d}t}\frac{1}{2}(\|w_{1,x}\|_2^2 + m\|w_{2,x}\|_2^2) \leqslant -\frac{N}{2}\frac{\mathrm{d}}{\mathrm{d}t}\|w_2\|_2^2 - \frac{r_a(0)}{2}\|w_{2,x}\|_2^2 + C_2(t) + C_3(t)\|w_{1,x}\|_2^2, \tag{2.21}$$

where

$$C_2(t) = \frac{|f(t)|^2 L}{4\delta_0} + \frac{\|s'\|_\infty^2}{16\delta_0}\|w_1\|_2^2 + \frac{C^2}{4\delta_0}(1+\|w_1\|_2^2)^2\|w_2\|_2^2, \tag{2.22}$$

$$C_3(t) = \frac{1}{16\delta_0}\|1-s\|_\infty^2, \tag{2.23}$$

and $\|(w_1,w_2)\|_2$ are bounded as in (2.11). Integrating (2.21) over $t\in[0,T]$, we find

$$m'\|(w_{1,x},w_{2,x})\|_2^2(T) + \frac{N}{2}\|w_2\|_2^2 \leqslant C_4 + \int_0^T C_2(t')\,\mathrm{d}t' + \int_0^T C_3(t')\|(w_1,w_2)_x\|_2^2, \tag{2.24}$$

where $m' \equiv \frac{1}{2}\min(1,m)$,

$$C_4 = \frac{1}{2}\max(1,m)\|(u_{0,x},u_{1,x})\|_2^2 + \frac{N}{2}\|u_1\|_2^2, \tag{2.25}$$

and the Gronwall inequality implies

$$\|(w_{1,x}, w_{2,x})\|_2^2(T) \leqslant \frac{1}{m'}\left(C_4 + \int_0^T C_2(t)\,\mathrm{d}t\right)\exp\left\{\frac{1}{m'}\int_0^T C_3(t)\,\mathrm{d}t\right\}. \tag{2.26}$$

We see from (2.4) that $w_{2,t} \in C([0,\infty); H^1([0,L]))$; hence the pressure $p \in C([0,\infty); H^3([0,L]))$ from (2.1). We have thus shown the following theorem.

Theorem 2.1. *Under the growth condition (1.4) and the initial boundary conditions (1.5) and (1.6), the model cochlear system (1.1)–(1.3) has unique global solutions:*

$$(u, u_t, p) \in C([0,\infty); (H^1([0,L]))^2 \times H^3([0,L])).$$

The estimates can be improved with the additional assumption:

$$s(x) \geqslant s_0 > 0, \quad \forall x \in [0,L], \qquad \|\epsilon_s\|_2 < \frac{3r_a(0)}{2L^{3/2}}. \tag{2.27}$$

Theorem 2.2 (growth bounds). *Under the additional assumption (2.27), the global solutions in theorem 2.1 satisfy the bounds*

$$\begin{aligned}
&\|(u,u_t)\|_2^2 + \int_0^t \|u_t\|_2^2(t')\,\mathrm{d}t' \leqslant a_1 + a_2\int_0^t |f(t')|^2\,\mathrm{d}t',\\
&\|(u_x,u_{x,t})\|_2^2 + \int_0^t \|u_{x,t}\|_2^2(t')\,\mathrm{d}t' \leqslant a_3 + a_4\int_0^t\left(1+\int_0^{t'}|f(t'')|^2\,\mathrm{d}t''\right)^3\mathrm{d}t',
\end{aligned} \tag{2.28}$$

for some positive constants a_i, $i = 1,2,3,4$.

Proof. Multiplying (2.3) by $s(x)w_1$, and (2.4) by w_2, adding the two expressions and integrating over $[0,L]$, we estimate using the Cauchy–Schwarz inequality,

$$\begin{aligned}
(sw_1, w_{1,t}) + (w_2, (Aw_2)_t) &= -\left(\int_x^L \mathrm{d}x'\int_0^{x'}\epsilon_s w_2\,\mathrm{d}x'', w_2\right)\\
&\quad -(rw_2, w_2) + (f(t)(x-L), w_2)\\
&\leqslant -\left(\int_0^x w_2(x')\,\mathrm{d}x', \int_0^x \epsilon_s(x')w_2(x')\,\mathrm{d}x'\right) - r_a(0)\|w_2\|_2^2 + f(t)(w_2,(x-L))\\
&\leqslant -\left(r_a(0) - \frac{2}{3}L^{3/2}\|\epsilon_s\|_2\right)\|w_2\|_2^2 + \delta\|w_2\|_2^2 + \frac{|f|^2}{4\delta}\|(x-L)\|_2^2.
\end{aligned} \tag{2.29}$$

Choose $2\delta = r_a(0) - \frac{2}{3}L^{3/2}\|\epsilon_s\|_2 > 0$ we find

$$\frac{1}{2}\frac{\mathrm{d}}{\mathrm{d}t}((sw_1,w_1) + (Aw_2,w_2)) \leqslant -\delta\|w_2\|_2^2 + \frac{|f|^2}{4\delta}\frac{L^3}{3}. \tag{2.30}$$

So

$$\frac{1}{2}((sw_1,w_1) + (Aw_2,w_2))(t) \leqslant -\delta\int_0^t \|w_2\|_2^2 + c_0 + c_1\int_0^t |f(t')|^2\,\mathrm{d}t'. \tag{2.31}$$

where $c_0 = \frac{1}{2}((sw_1,w_1) + (Aw_2,w_2))(0)$, and $c_1 = L^3/12\delta$. Hence,

$$\begin{aligned}
&\frac{\min(s_0,m)}{2}\|(w_1,w_2)\|_2^2 \leqslant c_0 + c_1\int_0^t |f(t')|^2\,\mathrm{d}t',\\
&\int_0^t \|w_2\|_2^2(t')\,\mathrm{d}t' \leqslant \delta^{-1}c_0 + \delta^{-1}\int_0^t |f(t')|^2\,\mathrm{d}t'.
\end{aligned} \tag{2.32}$$

In particular, if $f(t)$ is a bounded continuous function, (2.32) gives the growth bounds:

$$\|(w_1, w_2)\|_2 \leqslant \mathrm{O}(t^{1/2}), \qquad \int_0^t \|w_2\|_2^2(t')\,\mathrm{d}t' \leqslant \mathrm{O}(t), \tag{2.33}$$

implying that $\|w_2\|_2$ has a bounded, time averaged L^2 norm square.

Similarly, we improve the gradient estimates. Multiplying (2.12) by $sw_{1,x}$, (2.13) by $w_{2,x}$ and integrating over $x \in [0, L]$, we cancel out the two integrals on $s(x)w_{1,x}w_{2,x}$. Proceeding as before, we arrive at:

$$\frac{\mathrm{d}}{\mathrm{d}t}\frac{1}{2}((sw_{1,x}, w_{1,x}) + m\|w_{2,x}\|_2^2) \leqslant -\frac{N}{2}\frac{\mathrm{d}}{\mathrm{d}t}\|w_2\|_2^2 - \frac{r_a(0)}{2}\|w_{2,x}\|_2^2 + C_2(t), \tag{2.34}$$

and so integrating over $[0, T]$ gives:

$$\begin{aligned}\frac{1}{2}((sw_{1,x}, w_{1,x}) + m\|w_{2,x}\|_2^2)(T) + \frac{r_a(0)}{2}\int_0^T \|w_{2,x}\|_2^2(t')\,\mathrm{d}t' + \frac{N}{2}\|w_2\|_2^2(T)\\ \leqslant \frac{1}{2}((su_{0,x}, u_{0,x}) + m\|u_{1,x}\|_2^2) + \frac{N}{2}\|u_1\|_2^2 + \int_0^T C_2(t')\,\mathrm{d}t'\\ \equiv C_{5,0} + \int_0^T C_2(t')\,\mathrm{d}t'.\end{aligned} \tag{2.35}$$

If $s(x) \geqslant s_0 > 0$, then,

$$\|(w_{1,x}, w_{2,x})\|_2^2(T) + \frac{r_a(0)}{2m''}\int_0^T \|w_{2,x}\|_2^2(t)\,\mathrm{d}t \leqslant \frac{1}{m''}\left(C_{5,0} + \int_0^T C_2(t)\,\mathrm{d}t\right), \tag{2.36}$$

where $m'' = \frac{1}{2}\min(s_0, m)$. Substituting (2.32) in (2.36) gives (2.28). In particular, for a bounded continuous $f(t)$,

$$\|(w_{1,x}, w_{2,x})\|_2^2(T) + \frac{1}{2m''}\int_0^T \|w_{2,x}\|_2^2(t)\,\mathrm{d}t \leqslant \mathrm{O}(T^3). \tag{2.37}$$

This completes the proof.

If the nonlinear damping functions are bounded, i.e. if

$$r_a(\xi) \leqslant C_6, \quad r_a'(\xi)\xi \leqslant C_6, \quad P(\xi) \leqslant C_6, \qquad \forall \xi \geqslant 0, \tag{2.38}$$

for some positive constant C_6, then we have the following theorem.

Theorem 2.3 (uniform bounds). *Under the assumptions (2.27) and (2.38), and that $f(t)$ is a bounded continuous function, the global solutions in theorem 2.1 are uniformly bounded:*

$$\|(u, u_t)\|_{H^1} + \|p\|_{H^3} \leqslant C_7 < \infty, \qquad \forall t \geqslant 0,$$

for some positive constant C_7. Moreover, the dynamics admit an absorbing ball:

$$\limsup_{t\to\infty}(\|(u, u_t)\|_{H^1} + \|p\|_{H^3}) \leqslant C_8,$$

where C_8 is independent of initial data.

See [21] for an example of a bounded damping function. The energy inequality (2.30) lacks a term like $-\mathrm{const}\|w_1\|_2^2$ on the right-hand side, and so is insufficient to provide uniform bounds. The idea is to bring out the skew symmetric part of the system.

Proof. Multiply (2.3) by mw_2, (2.4) by w_1, integrate over $x \in [0, L]$, and add the resulting expressions to get

$$\begin{aligned}m(w_1, w_2)_t + (\tilde{A}w_{2,t}, w_1) = m\|w_2\|_2^2 - (sw_1, w_1) - (rw_2, w_1)\\ +(f(t)(x - L), w_1) - \left(w_1, \int_x^L \mathrm{d}x' \int_0^{x'} \epsilon_s w_2\,\mathrm{d}x''\right).\end{aligned} \tag{2.39}$$

Using the identity

$$\frac{\mathrm{d}}{\mathrm{d}t}(\tilde{A}w_2, w_1) = (\tilde{A}w_{2,t}, w_1) + (\tilde{A}w_2, w_{1,t}) = (\tilde{A}w_{2,t}, w_1) + (\tilde{A}w_2, w_2),$$

we have

$$\begin{aligned}\frac{\mathrm{d}}{\mathrm{d}t}[m(w_1, w_2) + (\tilde{A}w_2, w_1)] &= (\tilde{A}w_2, w_2) + m\|w_2\|_2^2 - (sw_1, w_1) - (rw_2, w_1)\\ &\quad +(f(t)(x-L), w_1) - \left(w_1, \int_x^L \mathrm{d}x' \int_0^{x'} \epsilon_s w_2 \,\mathrm{d}x''\right)\\ &\leqslant (NL^2 + m)\|w_2\|_2^2 - s_0\|w_1\|_2^2 + C_6\|w_2\|_2\|w_1\|_2\\ &\quad +|f|L^{3/2}\|w_1\|_2 + L^{3/2}\|\epsilon_2\|_2\|w_1\|_2\|w_2\|_2. \end{aligned} \tag{2.40}$$

Applying the Cauchy–Schwarz to polarize the last three terms we get

$$\begin{aligned} C_6\|w_2\|_2\|w_1\|_2 &\leqslant \frac{C_6^2}{s_0}\|w_2\|_2^2 + \frac{s_0}{4}\|w_1\|_2^2,\\ |f|L^{3/2}\|w_1\|_2 &\leqslant \frac{|f|^2L^3}{s_0} + \frac{s_0}{4}\|w_1\|_2^2,\\ L^{3/2}\|\epsilon_2\|_2\|w_1\|_2\|w_2\|_2 &\leqslant \frac{L^3\|\epsilon_2\|_2^2}{s_0}\|w_2\|_2^2 + \frac{s_0}{4}\|w_1\|_2^2. \end{aligned} \tag{2.41}$$

It follows from (2.40) that

$$\frac{\mathrm{d}}{\mathrm{d}t}[m(w_1, w_2) + (\tilde{A}w_2, w_1)] \leqslant C_9\|w_2\|_2^2 - \frac{s_0}{4}\|w_1\|_2^2 + \frac{|f|^2L^3}{s_0}, \tag{2.42}$$

where

$$C_9 = NL^2 + m + \frac{C_6^2}{s_0} + \frac{L^3\|\epsilon_2\|_2^2}{s_0}.$$

Multiplying (2.30) by a positive constant C_p and adding the resulting inequality to (2.42), we find

$$\frac{\mathrm{d}}{\mathrm{d}t}E_p \leqslant (-\delta C_p + C_9)\|w_2\|_2^2 - \frac{s_0}{4}\|w_1\|_2^2 + |f|^2\left(\frac{L^3}{s_0} + \frac{C_pL^3}{12\delta}\right), \tag{2.43}$$

where

$$E_p = \frac{C_p}{2}((sw_1, w_1) + (Aw_2, w_2)) + m(w_1, w_2) + (\tilde{A}w_2, w_1).$$

Choose C_p large enough such that $C_p > C_9/\delta$, and

$$E_p \leqslant \frac{3C_p}{4}((sw_1, w_1) + (Aw_2, w_2)) \leqslant \frac{3C_p}{4}\max(\|s\|_\infty, m + NL^2)\|(w_1, w_2)\|_2^2.$$

On the other hand,

$$\begin{aligned} E_p &\geqslant \frac{C_p}{4}((sw_1, w_1) + (Aw_2, w_2))\\ &\geqslant \min(s_0, m)\frac{C_p}{4}\|(w_1, w_2)\|_2^2. \end{aligned} \tag{2.44}$$

Then, for some positive constant C_{10},

$$\frac{\mathrm{d}}{\mathrm{d}t}E_p \leqslant -C_{10}E_p + |f|^2\left(\frac{L^3}{s_0} + \frac{C_pL^3}{12\delta}\right). \tag{2.45}$$

The uniform bound on $\|(u, u_t)\|_2$ follows from (2.45). Moreover, the fact that C_{10} is independent of initial data implies the absorbing ball property of (u, u_t) in L^2 (i.e. the limsup

as $t \to \infty$ is bounded, independent of initial data). Equation (2.4) and the L^2 invertibility of the operator A imply a similar uniform bound on u_{tt}. Equation (2.1) in turn shows that $\|p\|_{H^2}$ is uniformly bounded and has the absorbing ball property as well.

Now, we proceed with the gradient estimate of (w_1, w_2). The symmetric inequality is just (2.34) but with C_2 now uniform in time. The skew symmetric inequality is obtained by multiplying $mw_{2,x}$ with (2.12) plus $w_{1,x}$ times (2.13), and integrating over $x \in [0, L]$:

$$\begin{aligned}\frac{\mathrm{d}}{\mathrm{d}t}[m(w_{1,x}, w_{2,x})] - N\left(w_{1,x}, \frac{\mathrm{d}}{\mathrm{d}t}\int_0^x w_2(x', t)\,\mathrm{d}x'\right)\\ \leqslant \left(w_{1,x}, \int_0^x \epsilon_s w_2\right) - (rw_{2,x}, w_{1,x}) - (s'w_1, w_{1,x}) - s_0\|w_{1,x}\|_2^2\\ + f(t)(1, w_{1,x}) + 2C_6(|w_{1,x}|, |w_{2,x}|) + C_{11}(|w_2|, |w_{1,x}|). \end{aligned} \tag{2.46}$$

The second term on the left-hand side is

$$N(w_1, w_{2,t}) = N\frac{\mathrm{d}}{\mathrm{d}t}(w_1, w_2) - N\|w_2\|_2^2.$$

It follows that

$$\frac{\mathrm{d}}{\mathrm{d}t}[m(w_{1,x}, w_{2,x}) + N(w_1, w_2)] \leqslant 4C_6\|w_{1,x}\|_2\|w_{2,x}\|_2 - \frac{s_0}{2}\|w_{1,x}\|_2^2 + C_{12}, \tag{2.47}$$

for a positive constant C_{12}; or,

$$\frac{\mathrm{d}}{\mathrm{d}t}[m(w_{1,x}, w_{2,x}) + N(w_1, w_2)] \leqslant \frac{16C_6^2}{s_0}\|w_{2,x}\|_2^2 - \frac{s_0}{4}\|w_{1,x}\|_2^2 + C_{12}. \tag{2.48}$$

Multiplying (2.34) by a constant $C_p' > 0$ with C_2 constant, and adding the resulting inequality to (2.48), we get

$$\frac{\mathrm{d}}{\mathrm{d}t}E_p' \leqslant -\frac{s_0}{4}\|w_{1,x}\|_2^2 + C_{13} - \left(\frac{C_p' r_a(0)}{2} - \frac{16C_6^2}{s_0}\right)\|w_{2,x}\|_2^2, \tag{2.49}$$

where

$$E_p' = \frac{C_p'}{2}((sw_{1,x}, w_{1,x}) + N\|w_2\|_2^2 + m\|w_{2,x}\|_2^2) + m(w_{1,x}, w_{2,x}) + N(w_1, w_2),$$

and $C_{13} = C_2C_p' + C_{12}$. The term (w_1, w_2) is bounded from above by a constant times $\|(w_{1,x}, w_{2,x})\|_2^2$ due to the Poincaré inequality and so we can choose

$$C_p' > \frac{32C_6^2}{s_0 r_a(0)},$$

large enough so that for some positive constants C_{14}, C_{14}':

$$C_{14}'\|(w_{1,x}, w_{2,x})\|_2^2 \geqslant E_p' \geqslant C_{14}\|(w_{1,x}, w_{2,x})\|_2^2. \tag{2.50}$$

Inequality (2.49) yields

$$\frac{\mathrm{d}}{\mathrm{d}t}E_p' \leqslant -C_{15}E_p' + C_{13}, \tag{2.51}$$

implying the uniform estimate on $\|(u_x, u_{t,x})\|_2$ and the absorbing ball property. The uniform estimate and absorbing ball property on $\|p\|_{H^3}$ follows from (2.4) and (2.1). The proof is complete.

Remark 2.1. The estimates in theorem 2.3 imply that the evolution map denoted by $S(t)$ is relatively compact in the space $(u, u_t) \in (L^2([0, L]))^2$. Hence, for any bounded initial data $(u, u_t)(0) \in (H^1([0, L]))^2$, the dynamics (u, u_t) approach, in the space $(L^2([0, L]))^2$, the universal attractor $\boldsymbol{A}$ defined as

$$\boldsymbol{A} = \bigcap_{t>0} S(t)B_{\rho_0},$$

where B_{ρ_0} denotes the ball of radius ρ_0 in $(H^1([0, L]))^2$, the absorbing ball given by the estimates of theorem 2.3.

3. Multi-tone solutions

In this section, we consider special solutions to (1.1)–(1.2) that exhibit explicitly their frequency contents. For simplicity, let us assume that $\epsilon_s(x) = 0$, and $s(x) \geqslant s_0 > 0$, $\forall\, x \in [0, L]$.

3.1. Linear waves

First, we consider the linear regime with $r = r_0$, a positive constant. Solutions are superpositions of single frequency time harmonic waves of the form $p = P(x)\,\mathrm{e}^{\mathrm{i}\omega t} + \text{c.c.}$, $u = U(x)\,\mathrm{e}^{\mathrm{i}\omega t} + \text{c.c.}$, where P and U are complex functions that satisfy

$$P = (-m\omega^2 + \mathrm{i}r_0\omega + s(x))U, \tag{3.1}$$

$$P_{xx} + N\omega^2 U = 0, \tag{3.2}$$

$$P_x(0) = P_{\text{in}},\ P(L) = 0. \tag{3.3}$$

Let

$$(\alpha + \mathrm{i}\beta)(x) = \frac{N\omega^2}{-m\omega^2 + \mathrm{i}r_0\omega + s(x)},$$

where both α and β are real; so,

$$(\alpha, \beta) = \frac{N\omega^2(-m\omega^2 + s(x), -r_0\omega)}{(-m\omega^2 + s(x))^2 + r_0^2\omega^2}. \tag{3.4}$$

Then, (3.1)–(3.3) is equivalent to

$$P_{xx} + (\alpha(x) + \mathrm{i}\beta(x))P = 0, \tag{3.5}$$

subject to (3.3). If $\omega \neq 0$, $\beta \neq 0$. We show the following lemma.

Lemma 3.1. *The boundary value problem, (3.5) and (3.3), has a unique solution for all ω such that $\|P\|_{H^2([0,L])} \leqslant C|P_{\text{in}}|$, for some constant C independent of ω.*

Proof. Write $P = P_{\text{in}}(x - L) + Q$; then, Q satisfies

$$Q_{xx} + (\alpha(x) + i\beta(x))Q = -(\alpha(x) + i\beta(x))(x - L)P_{\text{in}} \equiv (f_1 + if_2)(x), \tag{3.6}$$

with boundary conditions $Q_x(0) = 0$, $Q(L) = 0$. The left-hand side is a Fredholm operator on Q, so it is sufficient to prove that zero is not an eigenvalue, which follows from the estimate below. Write $Q = q_1 + \mathrm{i}q_2$, then,

$$\begin{pmatrix} q_1 \\ q_2 \end{pmatrix}_{xx} + \begin{pmatrix} \alpha & -\beta \\ \beta & \alpha \end{pmatrix} \begin{pmatrix} q_1 \\ q_2 \end{pmatrix} = \begin{pmatrix} f_1 \\ f_2 \end{pmatrix}. \tag{3.7}$$

Multiplying (3.7) by $(q_2, -q_1)$, we find

$$q_{1,xx}q_2 - q_1q_{2,xx} - \beta q_2^2 - \beta q_1^2 = f_1q_2 - f_2q_1,$$

which gives upon integrating over $x \in [0, L]$ and integrating by parts

$$-\int_0^L \beta(q_1^2 + q_2^2)\,\mathrm{d}x = \int_0^L (f_1q_2 - f_2q_1)\,\mathrm{d}x. \tag{3.8}$$

Multiplying (3.7) by (q_1, q_2), integrating over $x \in [0, L]$, we have after integration by parts

$$-\|(q_{1,x}, q_{2,x})\|_2^2 + \int_0^L \alpha(q_1^2 + q_2^2) = \int_0^L (f_1 q_1 + f_2 q_2). \tag{3.9}$$

It follows from (3.9) and the Poincaré inequality that

$$\begin{aligned}\|(q_1, q_2)\|_2^2 &\leqslant L^2 \|(q_{1,x}, q_{2,x})\|_2^2 \\ &\leqslant L^2 \|\alpha\|_\infty \|(q_1, q_2)\|_2^2 + L^2 \|(f_1, f_2)\|_2 \|(q_1, q_2)\|_2. \end{aligned} \tag{3.10}$$

For $|\omega| \leqslant \omega_0 \ll 1$, $\|\alpha\|_\infty \leqslant 2N\omega^2/s_0$, $2\omega^2 L^2 N/s_0 \leqslant \frac{1}{2}$,

$$\|(q_1, q_2)\|_2 \leqslant 2L^2 \|(f_1, f_2)\|_2. \tag{3.11}$$

As $\|(f_1, f_2)\|_2 = \mathrm{O}(\omega^2)$, (3.11) implies $\|(q_1, q_2)\|_2 = \mathrm{O}(\omega^2)$ for $\omega \ll 1$. For $\omega^2 \geqslant M = M(N, m, s, r_0)$, M large enough, $\alpha \sim -N/m$, (3.9) shows

$$\|(q_1, q_2)\|_2 \leqslant \frac{2m}{N} \|(f_1, f_2)\|_2. \tag{3.12}$$

When $\omega_0^2 \leqslant \omega^2 \leqslant M$, $|\beta|$ is bounded from below uniformly in ω:

$$|\beta| \geqslant \frac{N r_0 |\omega|^3}{\|-m\omega^2 + s(x)\|_\infty^2 + r_0^2 \omega^2} \geqslant \beta_0,$$

for some positive constant β_0 only depending on r_0, m, L, and $s(x)$. Inequality (3.8) gives

$$\|(q_1, q_2)\|_2 \leqslant \beta_0^{-1} \|(f_1, f_2)\|_2 = \beta_0^{-1} C_1(N, m, r_0, L, s) |P_{\mathrm{in}}|, \tag{3.13}$$

for a positive constant $C_1(N, m, r_0, L, s)$, uniformly in $\omega^2 \in [\omega_0^2, M]$. Combining (3.11)–(3.13), we see that for any ω, and any given P_{in}, there is a unique solution P, $\|P\|_2 \leqslant C_2 |P_{\mathrm{in}}|$, for constant C_2 independent of ω. The lemma is proved by applying the L^2 estimate and the P equation (3.5).

3.2. Nonlinear waves

We are interested in the persistence of multi-tone solutions when nonlinearities are present. For simplicity, we shall consider: (A1) $r_a > 0$, a constant, and $P(u) = u^2$, the overall nonlinearity is cubic. As for linear waves, assume that (A2) $\epsilon_s = 0$, $s(x) \geqslant s_0 > 0$, $s \in C^1([0, L])$. We prove the following theorem.

Theorem 3.1 (existence and uniqueness of multi-tone solutions). *Let the left boundary condition be*

$$f_{\mathrm{in}}(t) = \sum_{j=1,\ldots,m} a_j \exp\{\mathrm{i}\omega_j t\} + \mathrm{c.c.},$$

and fix $\rho \geqslant 1$. Then, under (A1)–(A2) and for γ small enough (independent of ρ), system (1.1)–(1.2) has a unique solution of the form:

$$u(x, t) = \sum_{k \in Z^m} U_k(x) \exp\{\mathrm{i}k \cdot \omega t\} + \mathrm{c.c.}, \tag{3.14}$$

where $\omega = (\omega_1, \omega_2, \ldots, \omega_m)$, and complex valued functions $U_k(x) \in H^1([0, L])$, such that

$$\|u\| \equiv \sum_k \rho^{|k|} \|U_k\|_{H^1} < \infty. \tag{3.15}$$

The pressure p is similar.

Proof. Let B be the Banach space consisting of space–time functions of the form (3.14) with norm (3.15). Let $B_1 = \{v \in B : v_t \in B\}$, a subspace of B. Consider the mapping $M : v \in B_1 \to u$ defined as the unique bounded solution of the following equation in B_1:

$$mu_{tt} + \int_x^L \mathrm{d}x' \int_0^{x'} \mathrm{d}x'' N u_{tt} + f_{\mathrm{in}}(t)(L - x) + r_a u_t + s(x)u = -\gamma r_{\mathrm{nl}}(x, v^2)v_t, \tag{3.16}$$

where γr_{nl} is the nonlinear nonlocal part of the damping function.

Let us show that M is a well-defined bounded mapping from B_1 to itself. First, we notice that for any functions $u_i \in B$, $i = 1, 2$:

$$\begin{aligned} u_1 \cdot u_2 &= \sum_{k_1 \in Z^m} u_{1,k_1} \mathrm{e}^{\mathrm{i}k_1 \cdot \omega t} \sum_{k_2 \in Z^m} u_{2,k_2} \mathrm{e}^{\mathrm{i}k_2 \cdot \omega t} \\ &= \sum_{j \in Z^m} \left(\sum_{k_1 + k_2 = j} u_{1,k_1} u_{2,k_2} \right) \mathrm{e}^{\mathrm{i}j \cdot \omega t}. \end{aligned}$$

So

$$\begin{aligned} \|u_1 u_2\| &= \sum_{j \in Z^m} \rho^{|j|} \left\| \sum_{k_1 + k_2 = j} u_{k_1} u_{k_2} \right\|_{H^1} \leqslant \sum_{k_1, k_2 \in Z^m} \rho^{|k_1| + |k_2|} \|u_{k_1} u_{k_2}\|_{H^1} \\ &= \sum_{k_1 \in Z^m} \rho^{|k_1|} \|u_{k_1}\|_{H^1} \sum_{k_2 \in Z^m} \rho^{|k_2|} \|u_{k_2}\|_{H^1} = \|u_1\| \|u_2\|. \end{aligned} \tag{3.17}$$

It follows that

$$\|r_{\mathrm{nl}}(x, v^2)v_t\| \leqslant C\|v^2 * K\| \|v_t\| \leqslant C'\|v^2\| \|v_t\| = C'\|v\|^2 \|v_t\|, \tag{3.18}$$

where C' depends on the kernel function K and $*$ denotes the convolution integral on $[0, L]$. Denoting $F(x, t) = -\gamma r_{\mathrm{nl}}(x, v^2)v_t \in B$, we show that $u \in B_1$. Write $F(x, t) = \sum_{k \in Z^m} F_k \, \mathrm{e}^{\mathrm{i}k \cdot \omega t} + \text{c.c.}$, then (3.16) is the same as the system

$$\begin{aligned} &p_{xx} - N u_{tt} = 0, \\ &p = mu_{tt} + r_a u_t + s(x)u + F, \end{aligned} \tag{3.19}$$

with boundary condition $p_x(0, t) = f_{\mathrm{in}}(t)$, $p(L, t) = 0$. We seek a solution of system (3.19) in the form

$$\begin{aligned} p &= \sum_{k \in Z^m} p_k \mathrm{e}^{\mathrm{i}k \cdot \omega t} + \text{c.c.}, \\ u &= \sum_{k \in Z^m} u_k \, \mathrm{e}^{\mathrm{i}k \cdot \omega t} + \text{c.c.}, \end{aligned}$$

resulting in ($k = (k_1, k_2, \ldots, k_m)$):

$$\begin{aligned} &p_k = (-m(k \cdot \omega)^2 + \mathrm{i}r_a(k \cdot \omega) + s(x))u_k + F_k, \\ &p_{k,xx} + N(k \cdot \omega)^2 u_k = 0, \end{aligned} \tag{3.20}$$

with boundary condition $p_k(L) = 0$, $p_{k,x}(0) = 0$ if k is not one of the m modes (along e_j, $j = 1, 2, \ldots, m$) of f_{in}; otherwise $p_{k,x}(0) = a_j$, if $k = e_j$.

For each k, the system (3.20) can be uniquely solved as in lemma 4.1, with the estimates

$$\begin{aligned} &\|p_k\|_{H^1} \leqslant C_1 \|F_k\|_2 + C_2 \|f_{in,k}\|_2, \\ &\|u_k\|_{H^1} \leqslant \frac{C_3 \|p_k\|_{H^1}}{(1 + |k \cdot \omega|)}. \end{aligned} \tag{3.21}$$

It follows that the mapping M is from B_1 to itself, and it is not difficult to check that M is a contraction mapping if γ is small enough. This completes the proof.

4. Numerical results

The model system is computed with a second-order semi-implicit finite difference method; we refer to [23] for details and choice of the coefficient functions in the model other than $P(u) = u^2$. The input at the left boundary $x = 0$ is the sum of two tones (sinusoids) at frequencies $f_1 = 3.5$ kHz (kiloHertz) and $f_2 = 4$ kHz, with amplitudes 80 dB (decibel) and 85 dB, respectively. The zero decibel is $20\,\mu$ Pa in physical units. The time step is 0.01 ms (millisecond) and the spatial grid is 0.01 cm. The computation ends at 20 ms when the BM responses reach a steadily oscillating state. To observe the frequency content of such a state, we select four points (x_js, $j = 1, 2, 3, 4$) on BM, and examine the response time series ($u(x_j, t)$) at these points from 5 ms to 20 ms (to omit initial transient effects). The power spectral density

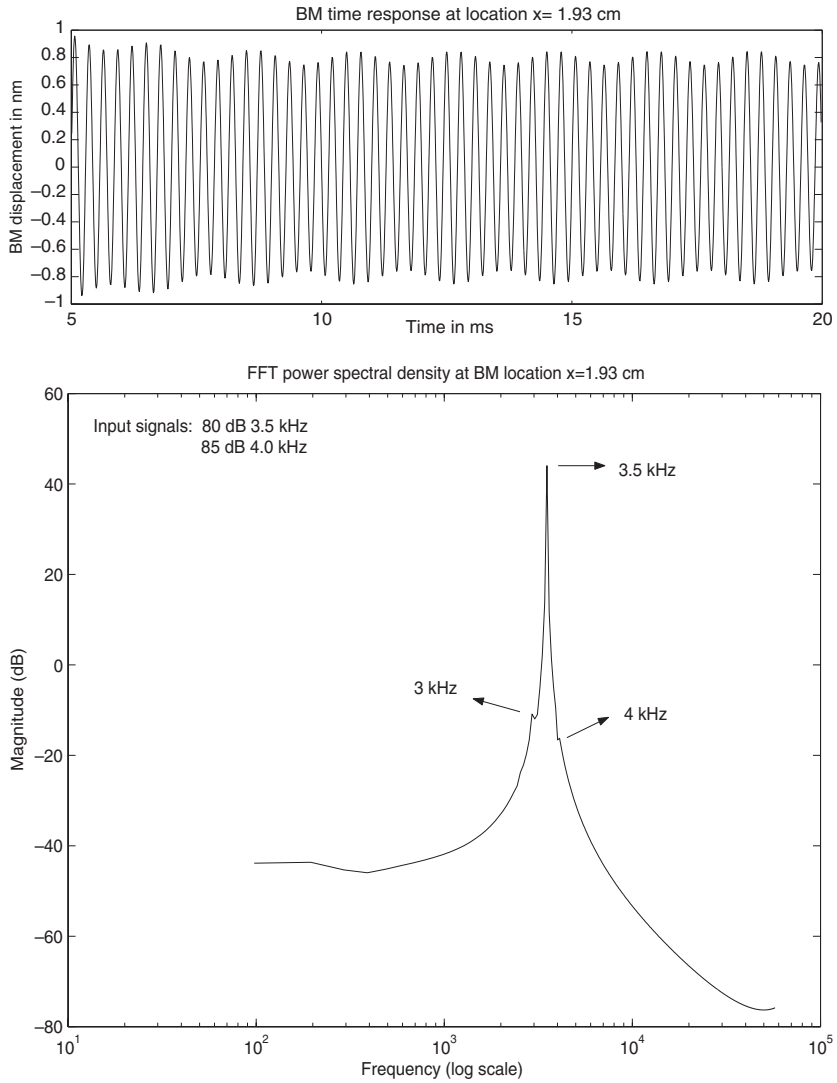

Figure 1. Time series of BM displacement at $x = 1.93$ cm (top frame), and its FFT power spectral density versus frequency (bottom frame).

of $u(x_j, t)$ at each j is obtained using the signal processing tool (sptool) in Matlab, to illustrate the energy distribution across frequencies on a log-scale.

Figure (1) (top frame) shows the time series of BM displacement at $x = 1.93$ cm; the bottom frame is the log–log plot of FFT power spectral density versus frequency. We see the major peak at 3.5 kHz, as $x = 1.93$ cm is the (so-called characteristic) location for the peak of a single 3.5 kHz tone. A characteristic location for a tonal input refers to the BM location of the maximal peak response at steady state. In addition, we see two small side peaks at 3 kHz ($= 2f_1 - f_2$), and 4 kHz (f_2). In figure 2, at $x = 1.85$ cm, the characteristic location for f_2, the f_2 peak is more pronounced; however, the f_1 peak is still the highest. Such a response of the lower frequency tone f_1 to a higher frequency tone f_2 is called upward masking in hearing.

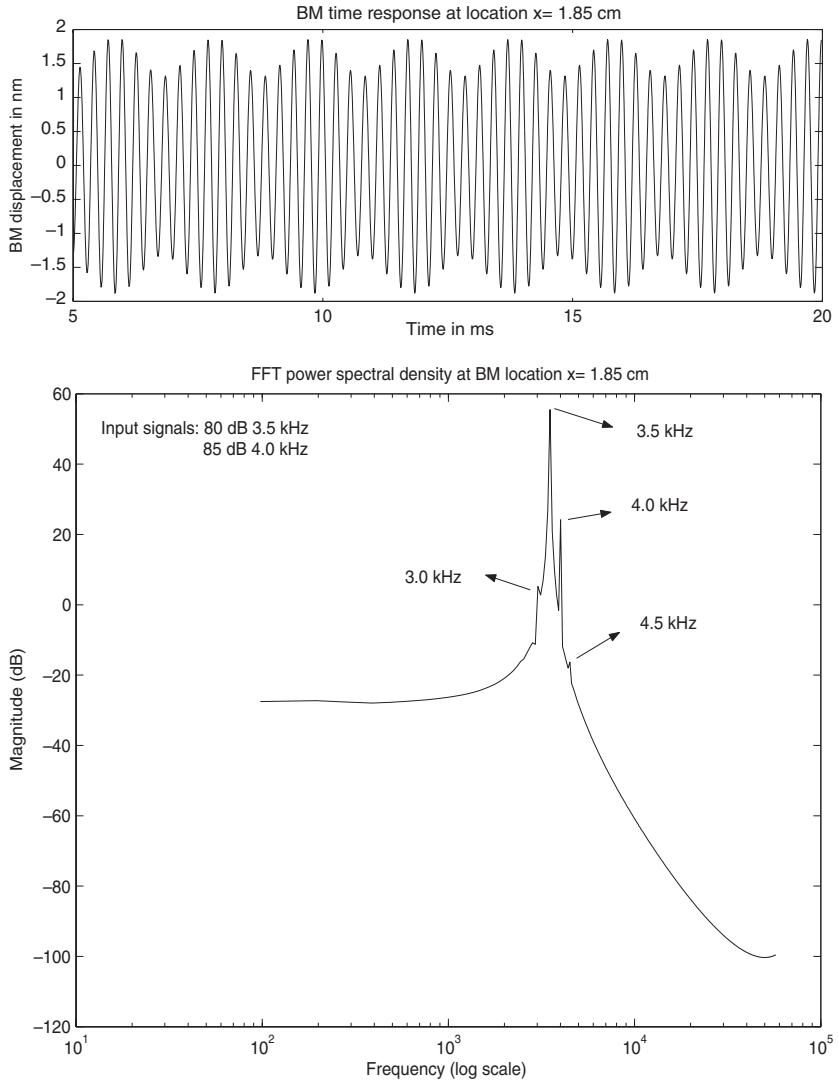

Figure 2. Time series of BM displacement at $x = 1.85$ cm (top frame), and its FFT power spectral density versus frequency (bottom frame).

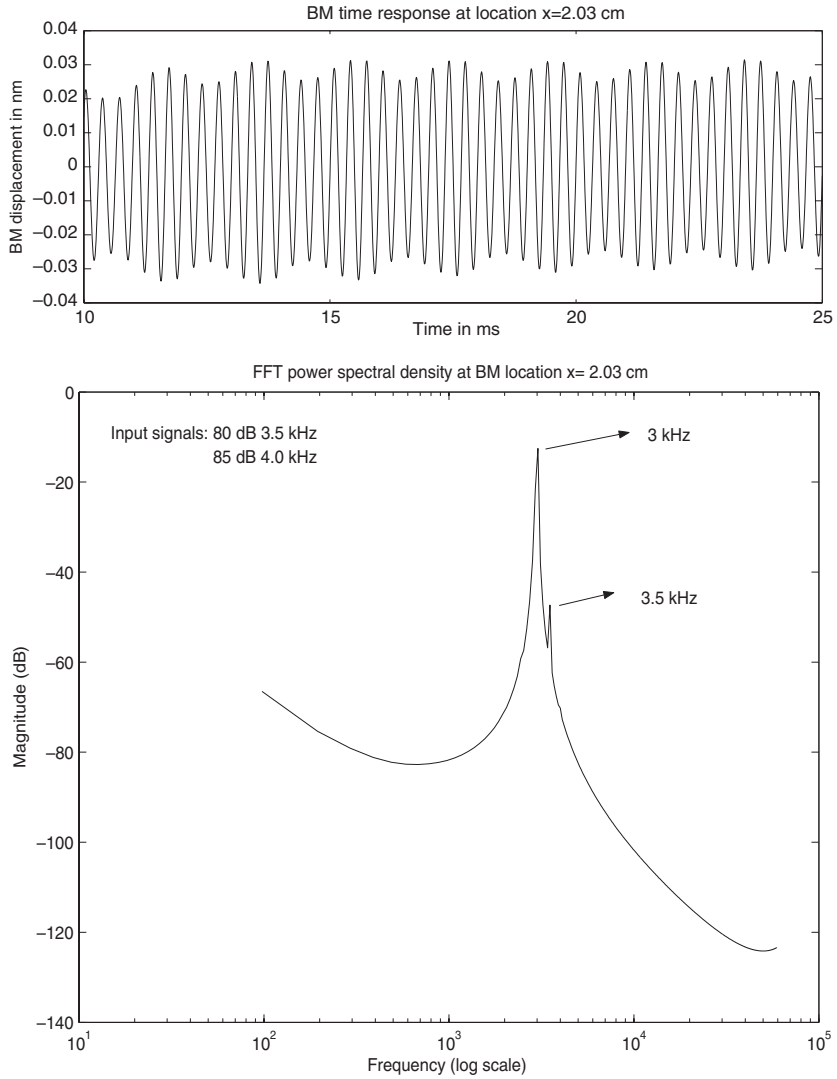

Figure 3. Time series of BM displacement at $x = 2.03$ cm (top frame), and its FFT power spectral density versus frequency (bottom frame).

In addition, there are two small side peaks at 3.0 kHz ($= 2f_1 - f_2$) and 4.5 kHz ($= 2f_2 - f_1$). In figure 3, at $x = 2.03$, the characteristic location for 3 kHz, a dominant single peak due to the generated combination tone $2f_1 - f_2$ is observed. In contrast, the $2f_2 - f_1$ tone ($= 4.5$ kHz) is weaker and dominated by f_1 and f_2 even at its characteristic location $x = 1.69$ cm (see figure (4)). The above findings on combination tones are consistent with the experiments on cochlea [19] and the analytic structures of multi-tone solutions in the previous section.

5. Conclusions

The nonlinear nonlocal cochlear models of the transmission line type are well-posed globally in time and admit exact multi-frequency solutions in the weakly cubic nonlinear regime. For

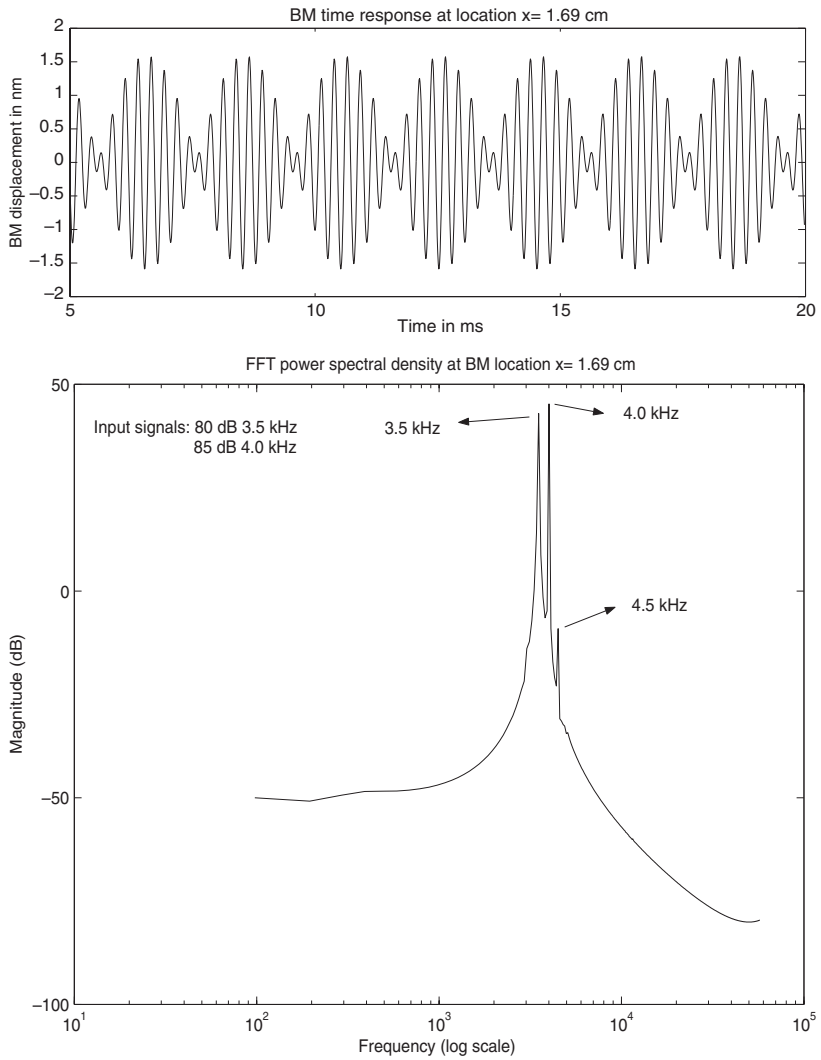

Figure 4. Time series of BM displacement at $x = 1.69$ cm (top frame), and its FFT power spectral density versus frequency (bottom frame).

finitely many tonal inputs at distinct frequencies, the exact solutions contain all integral linear combinations of input frequencies. For a two tone input with frequencies f_1 and f_2 at high enough intensities, we observed numerically the combination tones $2f_1 - f_2$ and $2f_2 - f_1$ in model output, in agreement with existing experimental observations [19] and the structure of analytical solutions.

Acknowledgments

JX would like to thank P Collet for a stimulating discussion of quasiperiodic solutions in dissipative systems, and a visiting professorship at the Inst. H Poincaré, where the work was in progress. He also thanks H Berestycki, P Constantin, G Papanicolaou, and J-M Roquejoffre for their interest.

Part of the work was done while YQ was an ICES (Institute of Computational Engineering and Sciences) visiting fellow at the University of Texas at Austin. The ICES research fellowship is gratefully acknowledged.

References

[1] Allen J B 1980 Cochlear modeling—1980 *Lecture Notes in Biomathematics* vol 43, ed M Holmes and L Rubenfeld (Berlin: Springer) pp 1–8
[2] Beyer R T 1998 *Sounds of Our Times: Two Hundred Years of Acoustics* (New York: AIP)
[3] de Boer E 1996 Mechanics of the cochlea: modeling efforts *Springer Handbook of Auditory Research* vol 8, ed P Dollas *et al* (Berlin: Springer) pp 258–317
[4] Deng L 1992 Processing of acoustic signals in a cochlear model incorporating laterally coupled suppresive elements *Neural Networks* **5** 19–34
[5] Deng L and Geisler C D 1987 Responses of auditory-nerve fibers to multiple-tone complexes *J. Acoust. Soc. Am.* **82** 1989–2000
[6] Geisler C D 1998 *From Sound to Synapse* (Oxford: Oxford University Press)
[7] Guinan J J and Peake W T 1967 Middle-ear characteristics of anesthesized cats *J. Acoust. Soc. Am.* **41** 1237–61
[8] Hall J L 1977 Two-tone suppression in a nonlinear model of the basilar membrane *J. Acoust. Soc. Am.* **61** 802–10
[9] Jau Y and Geisler C D 1983 Results from a cochlear model utilizing longitudinal coupling *Mechanics of Hearing* ed E de Boer and M Viergever (Dordrecht: Martinus Nijhoff) pp 169–76
[10] Keller J B and Neu J C 1985 Asymptotic analysis of a viscous cochlear model *J. Acoust. Soc. Am.* **77** 2107–10
[11] Kim D O 1986 An overview of nonlinear and active models *Lecture Notes in Biomathematics: Peripheral Auditory Mechanisms* vol 64, ed J Allen *et al* (Berlin: Springer) pp 239–49
[12] Leveque R, Peskin Ch and Lax P 1988 Solution of a two-dimensional cochlear model with fluid viscosity *SIAM J. Appl. Math.* **48** 191–213
[13] Liberman M C 1982 The cochlear frequency map for the cat: labeling auditory nerve fibers of known characteristic frequency *J. Acoust. Soc. Am.* **72** 1441–9
[14] Lyon R 1982 A computational model of filtering, detection, and compression in the cochlear *IEEE Int. Conf. Acoustics, Speech and Signal Processing* pp 1282–5
[15] Meddis R, O'Mard L, Lopez-Poveda E 2001 A computational algorithm for computing nonlinear auditory frequency selectivity *J. Acoust. Soc. Am.* **109** 2852–61
[16] Neely S 1985 Mathematical modeling of cochlear mechanics *J. Acoust. Soc. Am.* **78** 345–52
[17] Osher S and Rudin L 1990 Feature-oriented image enhancement using shock filters *SIAM J. Numer. Anal.* **27** 919–40
[18] Pohlmann K 2000 *Principles of Digital Audio* 4th edn (New York: McGraw-Hill Video/Audio Professional)
[19] Robles L and Ruggero M 2001 Mechanics of the mammalian cochlea *Physiol. Rev.* **81** 1305–52
[20] Sondhi M 1980 The acoustical inverse problem for the cochlea *Lecture Notes in Biomathematics* vol 43, ed M Holmes and L Rubenfeld (Berlin: Springer) pp 95–104
[21] Strube H W 1985 A computationally efficient basilar-membrane model *Acustica* **58** 207–14
[22] von Békésy G 1960 *Experiments in Hearing* (New York: McGraw-Hill)
[23] Xin J, Qi Y-Y and Deng L 2003 Time domain computation of a nonlinear nonlocal cochlear model with applications to multitone interaction in hearing *Commun. Math Sci.* **1** 211–27 (www.intlpress.com/CMS)
[24] Zeidler E 1995 *Applied Functional Analysis: Main Principles And Their Applications* (New York: Springer)